Mutations in *GDI1* are responsible for X-linked non-specific mental retardation

Patrizia D'Adamo[1], Andrea Menegon[2], Cristiana Lo Nigro[3], Marina Grasso[3], Massimo Gulisano[2], Filippo Tamanini[1], Thierry Bienvenu[4], Agi K. Gedeon[5], Ben Oostra[6], Shih-Kwang Wu[7], Anurag Tandon[7], Flavia Valtorta[2,8], William E. Balch[7], Jamel Chelly[4] & Daniela Toniolo[1,2]

Rab GDP-dissociation inhibitors (GDI) are evolutionarily conserved proteins that play an essential role in the recycling of Rab GTPases required for vesicular transport through the secretory pathway. We have found mutations in the *GDI1* gene (which encodes αGDI) in two families affected with X-linked non-specific mental retardation. One of the mutations caused a non-conservative substitution (L92P) which reduced binding and recycling of RAB3A, the second was a null mutation. Our results show that both functional and developmental alterations in the neuron may account for the severe impairment of learning abilities as a consequence of mutations in *GDI1*, emphasizing its critical role in development of human intellectual and learning abilities.

Introduction

Mental retardation is a common condition affecting about 3% of the human population. The disorder has a major genetic component, and defining the genes involved would be a major advance in terms of understanding brain functions important for development of intellectual and learning abilities. X-linked forms of mental retardation (XLMR) have been described[1]. In some cases, the mental retardation phenotype is part of a complex syndrome, but in many instances mental retardation is the only symptom and is known as non-specific mental retardation (MRX). There is no additional consistent feature to distinguish MRX patients from unaffected relatives or affected males in different families. The gene associated with the most common form of syndromic mental retardation, the Fragile X-A (FRAXA) syndrome is FMR1 (ref. 2) and shown to account for 15–20% of all XLMR (ref. 3). The remaining mentally retarded males, approximately 1 in 500, are a very heterogeneous group[1]. Approximately 50 MRX loci corresponding to individual families are mapped along the X chromosome and can be grouped in 8–10 non overlapping regions, suggesting the involvement of a minimum number of 8–10 X-linked genes[4]. Only one gene involved in MRX has been identified: loss of expression of *FMR2*, a gene of unknown function adjacent to the fragile X-E (FRAXE) site on Xq28, is consistently correlated with FRAXE expansion[5] in some mild mentally retarded patients.

Six families affected with MRX have been mapped in a gene-rich region of 8–9 cM in Xq28 (ref. 1). Among the genes within this interval which are predominantly or highly expressed in brain[6] is *GDI1*, which encods αGDI, one of the closely related isoforms of GDI. Members of the GDI family control the recycling of the Rab GTPases involved in membrane traffic[7,8]. GDI retrieves the GDP-bound form of Rab from the membrane to form a heterodimeric complex which serves as a cytosolic reservoir for the reuse of inactive Rab during multiple rounds of vesicle budding and fusion[9]. Because the Rab3 proteins play an important role in neurotransmitter release and are substrates for GDI[10–16], *GDI1* was a potential candidate for MRX.

Results

Mutation detection in *GDI1*

To test whether *GDI1* is responsible for mental retardation, families MRX3, MRX25, MRX28, MRX41 and MRX48 (ref. 1) were examined. From the cDNA and genomic sequence of *GDI1* (refs 6,17,18), the structure of the gene was established and primers were designed for direct sequencing of all coding exons and exon-intron junctions of PCR products prepared from RNA or genomic DNA of one patient from each family.

Mutations in *GDI1* were found in patients from two families, MRX48 (ref. 19) and MRX41 (ref. 20) (Fig. 1). Affected and non-affected relatives and obligate carriers were analysed and the mutations were shown to segregate with the disease by sequence

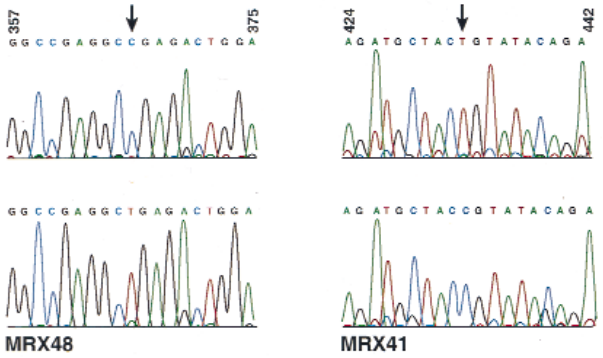

Fig. 1 Mutations in patients MRX41 and MRX48. The upper panels show the corresponding sequence from a normal individual; the lower panels are from the patients. Numbers correspond to nucleotide positions in the cDNA. Arrows point to the mutations.

[1]*Institute of Genetics Biochemistry and Evolution, CNR, Pavia, Italy.* [2]*DIBIT-HSR, Milano, Italy.* [3]*Laboratory of Human Genetics, Galliera Hospital, Genova, Italy.* [4]*Institute Cochin de Genetique Moleculaire, Paris, France.* [5]*Department of Cytogenetics and Molecular Genetics, Women's and Children's Hospital, North Adelaide, Australia.* [6]*Department of Clinical Genetics, Erasmus University, Rotterdam, The Netherlands.* [7]*Department of Molecular and Cell Biology, The Scripps Research Institute, La Jolla, California, USA.* [8]*Department of Medical Pharmacology, University of Milano, Milano, Italy. Correspondence should be addressed to D.T. e-mail: Toniolo@igbe.pv.cnr.it*

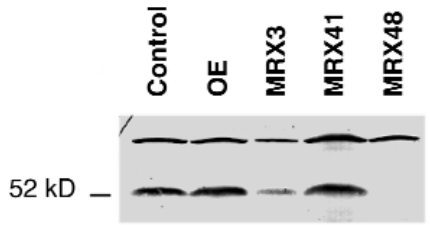

Fig. 2 Western-blot analysis of αGDI in a normal individual and MRX patients. Total proteins were extracted from approximately 3×10^6 lymphoblasts and fractionated on 10% SDS-PAGE gels. The 52-kD band corresponds to αGDI. The upper band is a non-specific band cross-reacting with the anti-αGDI antibody[21].

analysis and restriction enzyme digestion (a novel *Dde*I site is introduced by the mutation in family MRX48; data not shown). Sequencing of 100 normal chromosomes from different ethnic groups demonstrated that the mutations were not common polymorphisms. The mutation in family MRX48 was a C→T transition at position 366 of the cDNA. The mutation introduced a premature stop codon (TGA; R70X) and the truncated message could possibly lead to synthesis of a putative peptide of 69 amino acids in length (which is likely to be unstable and degraded). Indeed, lymphoblasts from MRX48 did not have any band corresponding to αGDI as determined by immunoblotting with anti-αGDI antibodies[21] (Fig. 2). The second mutation, in the MRX41 family, was a T→C transition at position 433 of the cDNA, causing a missense mutation and a non-conservative amino-acid change (L92P). Protein expression in lymphoblasts was comparable to normal individuals (Fig. 2).

No mutations were found by sequence analysis of *GDI1* in patients from families MRX3, 25, 28 or in a patient affected with mental retardation and progressive spastic paraplegia mapped to Xq28 (patient OE; ref. 22). Levels of αGDI in lymphoblasts from patients MRX3 and OE were very similar to those in control cells (Fig. 2), thus excluding mutations in regulatory regions with dramatic consequences on expression.

To determine the frequency of mutations in *GDI1* among mentally retarded patients, an unmapped population of mentally retarded FRAXA-negative males with normal karyotype was studied: 34 were familial cases, 55 were sporadic. Primers were used to amplify each exon for SSCP analysis, which was carried out under two different experimental conditions. A common polymorphism which did not change the amino-acid sequence was repeatedly found in exon 3 (A377C), but no additional mutations were found.

The missense mutation L92P alters RAB3A binding

The X-ray structure of αGDI (ref. 23) reveals that highly conserved residues in the *GDI* family and the closely related choroideremia (*CHM*) gene family involved in Rab prenylation[24] form a Rab-binding platform at the top of αGDI (refs 7,23; Fig. 3*a*). Mutation of residues forming the platform can lead to a greater than 60-fold decrease in Rab binding and concomitant loss of function in Rab3 recycling. The L92P mutation found in the MRX41 family affects a conserved residue in the α-helix beneath the Rab-binding platform and adjacent to a hydrophobic pocket potentially involved in binding of the geranylgeranyl group attached to the C terminus of Rab proteins (Fig. 3*a*). To determine whether the L92P substitution affects interaction with RAB3A, we generated mutant αGDI[L92P] by site-directed mutagenesis, expressed it in *Escherischia coli*, purified it to homogeneity, and examined its ability to bind RAB3A *in vitro*[23]. The protein was recognized by αGDI specific antibodies suggesting its overall structure was intact. Whereas RAB3A binds to wild-type αGDI with a K_d of 0.45 μM, the L92P substitution led to a 6.3 fold (K_d = 2.8 μM) decrease in affinity for RAB3A (Fig. 3*b*). This result suggested that the mutant αGDI may not be able to efficiently recycle Rab proteins *in vivo*. Consistent with this, the L92P mutant had reduced ability to extract Rab3a from rat brain synaptosomes (Fig. 3*c*). Moreover, expression of a homologous mutation in the yeast homologue *Gdi1p* (ref. 25) showed a recessive phenotype in the presence of wild-type *Gdi1p*, but had a moderate temperature-sensitive growth phenotype in a strain lacking wild-type *Gdi1p* (Δ*gdi1*) (S.K.W., P.L. & W.E.B., unpublished observation). The observed temperature-sensitivity may reflect decreased stability in protein folding at the elevated temperature. The introduction of the helix-breaking proline residue at position 92 may either indirectly destabilize the adjacent Rab-

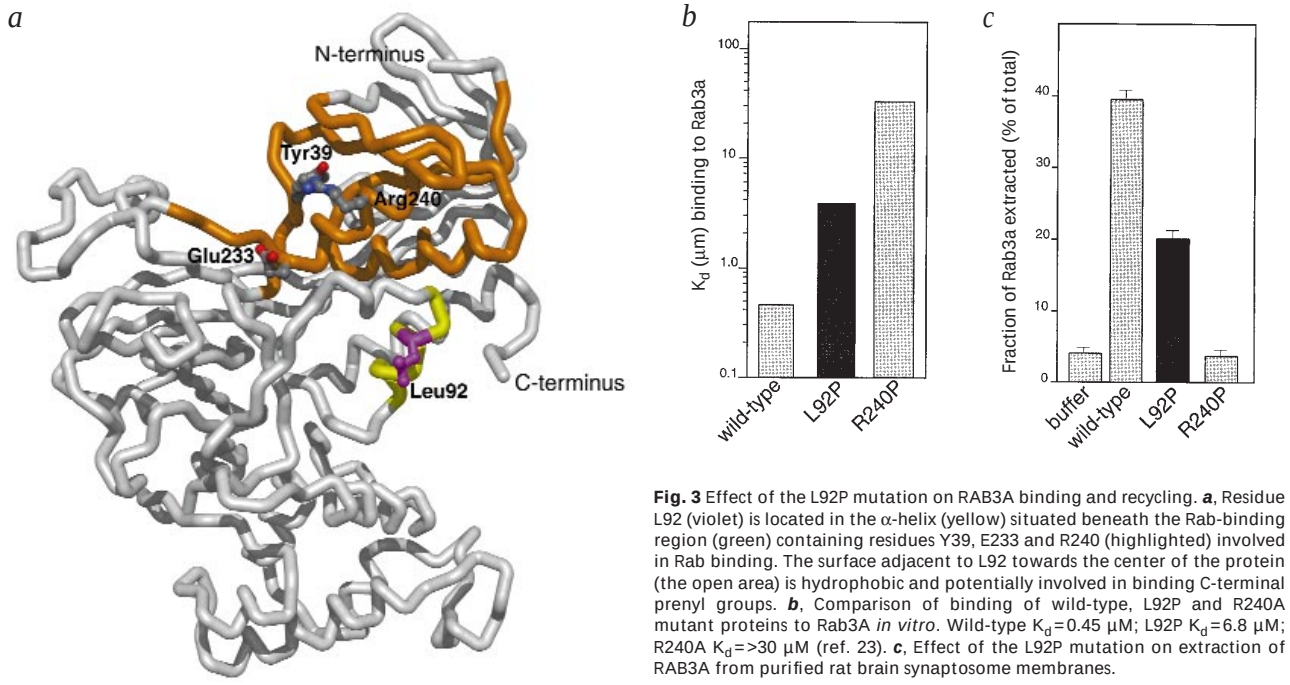

Fig. 3 Effect of the L92P mutation on RAB3A binding and recycling. ***a***, Residue L92 (violet) is located in the α-helix (yellow) situated beneath the Rab-binding region (green) containing residues Y39, E233 and R240 (highlighted) involved in Rab binding. The surface adjacent to L92 towards the center of the protein (the open area) is hydrophobic and potentially involved in binding C-terminal prenyl groups. ***b***, Comparison of binding of wild-type, L92P and R240A mutant proteins to Rab3A *in vitro*. Wild-type K_d = 0.45 μM; L92P K_d = 6.8 μM; R240A K_d = >30 μM (ref. 23). ***c***, Effect of the L92P mutation on extraction of RAB3A from purified rat brain synaptosome membranes.

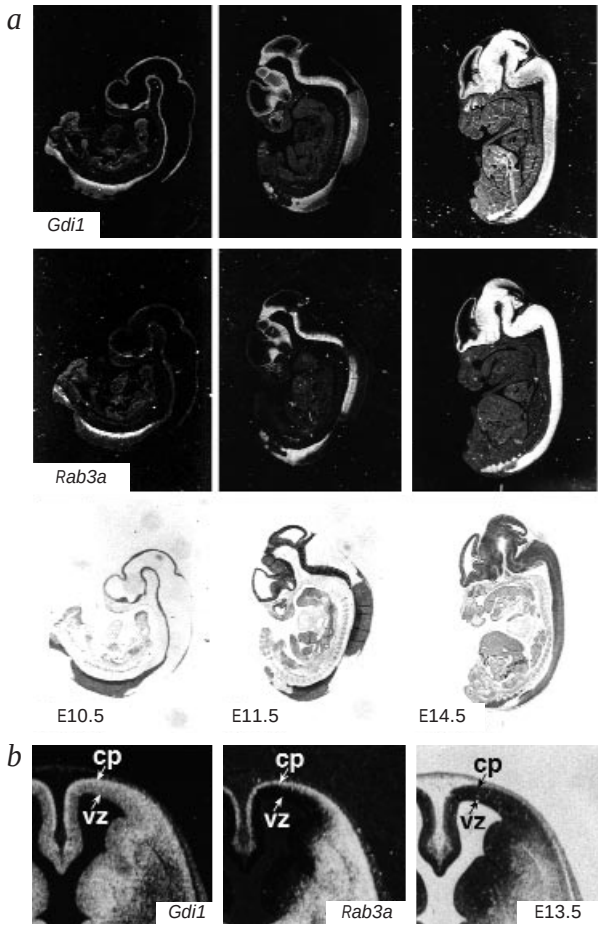

Fig. 4 *Gdi1* expression during mouse brain development. ***a***, *Gdi1* and *Rab3a* expression in mouse sagittal sections. Developmental age is indicated. Anterior is to the left. Lower panels are bright field views of the sections above counterstained with cresyl violet. ***b***, *Gdi1* and *Rab3a* expression in mouse transverse sections through an E13.5 brain at the level of the telencephalic vesicles. Anterior is up. A bright-field view of one of the sections counterstained with cresyl violet is also shown. While *Rab3a* is spatially restricted to the post-mitotic regions in the telencephalic cortex (cp, cortical plate), *Gdi1* is faintly expressed also in the proliferative layer (vz, ventricular zone). Sense probes gave no specific hybridization signals (data not shown).

binding region or reduce the ability of αGDI to recognize the carboxy-terminal prenyl group required for high-affinity binding during recycling (Fig. 3*a*).

A possible role of αGDI in neuronal development

In addition to their role in neurotransmitter release at the synapse[10–16], Rab proteins regulate vesicular traffic throughout the exocytic and endocytic pathways[26]. This ubiquitous function suggested that in neural tissues αGDI also may be necessary, and that impairment of such a putative function may be the cause of mental retardation. Furthermore, *GDI1* expression is upregulated during brain development in the postmitotic cell layers[27], presumably before synapses differentiate. We have compared the expression of the mouse homologue of *GDI1* with that of *Rab3a* by hybridization to adjacent saggital and transverse embryo sections at different stages of mouse development (Fig. 4*a*). Both *Gdi1* and *Rab3a* mRNA were first detectable at embryonic day (E) 9, when they were expressed in the ventral spinal cord at the caudal part of the embryo (Fig. 4*a*). From that stage on, both *Gdi1* and *Rab3a* were highly expressed in post-mitotic cells of neural tissues. Expression of *Rab3a* was limited to the post-mitotic cell layer while faint expression of *Gdi1* could be detected also in the proliferating ventricular zone (Fig. 4*b*). In postnatal brain (data not shown), the two genes continued to show a superimposable distribution in most of the brain regions characterized by high synaptic activity.

The pattern of *Gdi1* expression during development is consistent with a role in neuronal differentiation. To examine the potential effects of the loss of αGDI in MRX48 patients, we suppressed *Gdi1* expression in cultured rat hippocampal neurons using antisense oligonucleotides[28,29]. Two different oligonucleotides complementary to sequences surrounding the initiation of translation of the rat *Gdi1* gene were able to reduce the levels of expression of *Gdi1* significantly, as judged by immunofluorescence (Fig. 5*b*, panels c and f). The faint residual signal in antisense-treated neurons might be ascribed to the persistence of βGDI, the ubiquitous form of the protein which is present in neurons at low levels[27]. Treatment with the antisense oligonucleotides did not affect viability of neurons, but the process of neurite extension was severely impaired (Fig. 5*a*, panels b and c). Thirty-six hours after plating, the total length of processes/cell was 720 ± 121 μm in control cells (or in cells treated with irrelevant oligonucleotides of the same length) and 294 ± 156 μm in antisense-treated cells ($P < 0.001$; Student's t test). The inhibition was fully reversible. Thirty-six hours after withdrawal of the antisense oligonucleotides, the total length of processes per cell reached 907 ± 283 μm (Fig. 5*a*, panels c and f).

When neurons were allowed to develop for 48 hours before adding the antisense oligonucleotides, we observed apparent withdrawal of the already extended processes during the 48 hours of antisense treatment (Fig. 5*b*, panels a and d). Under these conditions, the total length of processes per cell was 48 ± 7% of that of control cells (600 ± 94 μm *versus* 1231 ± 111 μm; $P < 0.001$; Fig. 5*c*). Because at this stage of development hippocampal neurons have already acquired a polarized phenotype, we investigated whether withdrawal affected all neuronal processes independently of their polarity. Neurons were fixed at various time-points after the addition of the antisense oligonucleotides and immunostained with antibodies against MAP2, a marker specific for the somatodendritic compartment. The total length of MAP2 processes per cell (Fig. 5*c*) appeared similar in antisense-treated (361 ± 79 μm) and in control cells (304 ± 33 μm), suggesting that upon suppression of *Gdi1* expression, retraction of developing processes occurred selectively for axons, leaving elongation of dendrites unaffected. In control cells, αGDI was ubiquitously distributed in cell bodies and developing processes, independently of their polarity. In antisense-treated cells, MAP-2 positive processes showed a strongly reduced, albeit not abolished, level of staining (Fig. 5*b*, panels c and f).

Control experiments were performed with sense oligonucleotides to either αGDI or βGDI. Sense oligonucleotides were completely ineffective when added to neurons after 48 hours of culture. Conversely, for unknown reasons, when added immediately after plating, sense oligonucleotides to αGDI, but not to βGDI, caused cell death.

Discussion

We report that *GDI1*, one of the genes involved in the control of cycling between active and inactive state of the Rab family, has a major role in mental disorder. Evidence for this hypothesis comes from the identification of two different mutations in *GDI1* in two familial cases of MRX, previously mapped to the same chromosomal localization, in Xq28 (ref. 6).

Sequence and protein analysis have identified one mutation (in family MRX48) which disrupts synthesis of αGDI by introducing a premature stop codon in the open reading frame. The mutation has a dominant phenotypic effect as carrier females in the family

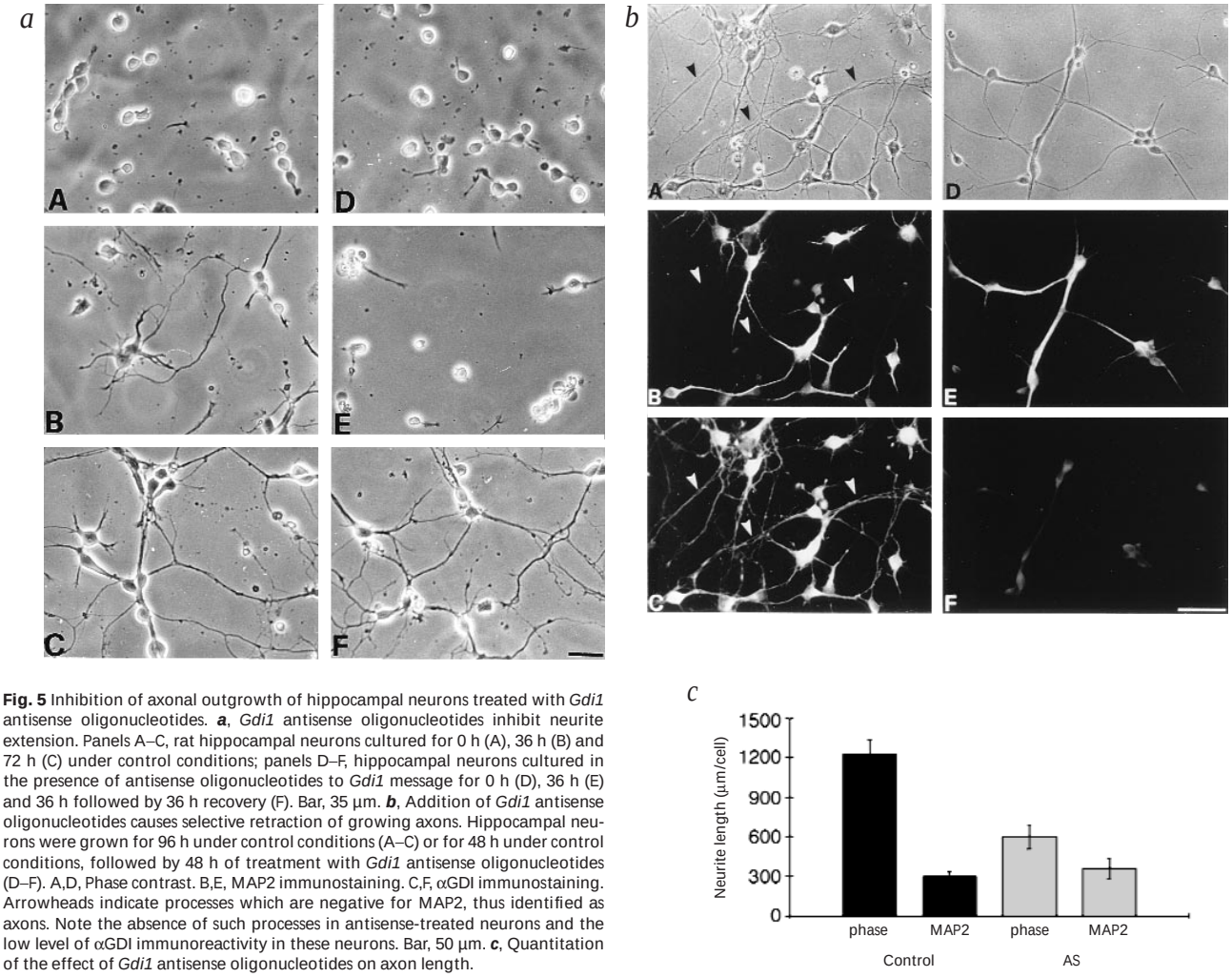

Fig. 5 Inhibition of axonal outgrowth of hippocampal neurons treated with *Gdi1* antisense oligonucleotides. ***a***, *Gdi1* antisense oligonucleotides inhibit neurite extension. Panels A–C, rat hippocampal neurons cultured for 0 h (A), 36 h (B) and 72 h (C) under control conditions; panels D–F, hippocampal neurons cultured in the presence of antisense oligonucleotides to *Gdi1* message for 0 h (D), 36 h (E) and 36 h followed by 36 h recovery (F). Bar, 35 µm. ***b***, Addition of *Gdi1* antisense oligonucleotides causes selective retraction of growing axons. Hippocampal neurons were grown for 96 h under control conditions (A–C) or for 48 h under control conditions, followed by 48 h of treatment with *Gdi1* antisense oligonucleotides (D–F). A,D, Phase contrast. B,E, MAP2 immunostaining. C,F, αGDI immunostaining. Arrowheads indicate processes which are negative for MAP2, thus identified as axons. Note the absence of such processes in antisense-treated neurons and the low level of αGDI immunoreactivity in these neurons. Bar, 50 µm. ***c***, Quantitation of the effect of *Gdi1* antisense oligonucleotides on axon length.

are also affected[18]. The second mutation (MRX41) alters a conserved residue (L92) in the α-helix beneath the Rab-binding platform and adjacent to the hydrophobic pocket potentially involved in binding of the geranylgeranyl group of Rab proteins[23]. The mutation L92P alters Rab recognition by αGDI as it reduces RAB3A binding more than sixfold and RAB3A extraction from rat brain synaptosomes. As carrier females in the family are not affected[19], it is likely that the residual αGDI activity in cells where the mutated X chromosome is active is sufficient for some vesicle cycling. Male phenotypes were similar in the two families.

Proteins of the GDI family bind to and retrieve the GDP-bound Rab proteins from membranes. In the brain, it is likely that the predominant role of αGDI is to bind RAB3A and RAB3C, the Rab3 proteins specific for or highly enriched in synapsis[10–16]. As a consequence, the major effect of both mutations could eventually be to greatly decrease the pool of Rab proteins available for synaptic vesicles cycling and neurotransmitter release. Ca^{2+}-triggered fusion of synaptic vesicles is altered in mice lacking Rab3a, due to a higher-than-usual number of exocytic events taking place after stimulation[30,31]. Our data suggest that mutations in *GDI1* could eventually also alter the exocytic events accompanying synaptic transmission.

The rather mild phenotype caused by the two mutations described here is consistent with the presence of other GDI isoforms which can perform a housekeeping role in Rab recycling, emphasizes a specialized role for αGDI in neurons and possibly in specific brain areas, and suggests that αGDI is essential for the normal function of Rab3 isoform(s). The striking, rather specific effects of loss of αGDI expression in the brain leading to MRX is not unlike the loss of the GDI-related protein CHM1 in choroideremia, a disease leading to selective retinal degeneration and blindness[32,33]. CHM1 is essential for the geranylation of a specific Rab protein (Rab27) required for maintenance of the pigmented retinal epithelium[33], while the second isoform, CHM2, may play a housekeeping role.

Our data also suggest an alternative or additional role for αGDI. Up regulation of expression of αGDI and RAB3A at the onset of brain differentiation, before any synaptic activity is detectable, and the specific inhibition of axonal (not dendritic) outgrowth in hippocampal neurons treated with *Gdi1* antisense oligonucleotides, suggest that αGDI may be essential for neuronal differentiation during brain development. The ubiquitous role of αGDI in vesicular traffic and its interaction with RAB3A as well as with other proteins of the Rab family can account for such an explanation. Lack of gross anatomical alterations in brain of MRX patients[18,19] do not exclude minor morphological but functionally important alterations in neuronal development.

Only two of the five families studied with linkage to Xq28 presented mutations in *GDI1*. While we cannot exclude that the phenotype of families MRX25 and MRX28 is related to mutations in regulatory regions of *GDI1*, protein analysis of lymphoblasts from the MRX3 and OE patients argues against such mutations and suggested at least one other MRX gene exists in Xq28. There are no obvert phenotypic differences between patients from these

five families, which suggests that the number of MRX genes may be higher than the 8-10 loci previously proposed. Such heterogeneity correlates quite well with the low frequency of mutations in *GDI1* among mentally retarded patients. We did not find mutations in the coding regions of *GDI1* among 89 male patients analysed by SSCP and Bienvenue *et al.* (personal communication) found one mutation among almost 200 patients analysed. The most common form of mental retardation, FRAXA, accounts for about 15% of all patients. The frequency of mutations in the genes responsible for all the remaining cases is likely to be very similar to that found for *GDI1*, namely less than 1%.

In summary, our data show that membrane traffic leading to neural development and function of the synapse is dependent on a specific role for αGDI. Disruption of its function leads to mental retardation in patients. Together with the genes associated with FRAXA and FRAXE, *GDI1* is one of the few genes shown to be involved in determining human intellectual abilities and the first that is not associated with a fragile site.

Note added in proof: While this manuscript was in press, disruption of a similar gene was reported in another set of MRX patients[42].

Methods

Sequence analysis. The entire coding region of the *GDI1* cDNA of patient MRX48 was amplified using primers P9 and 13 using the Expand Long Template PCR System (Boehringer) according to the manufacturer's instructions. RT-PCR was done as described[34]. Sequences of the MRX41 patient were deduced from PCR products of genomic DNA. Primers P9 and 17 were used to amplify the 5' moiety, primers 19 and 13 to amplify the 3' moiety, with the Expand Long Template PCR System. PCR conditions: 30 s at 96 °C, 30 s at 61°C or 63 °C, 3 min at 68 °C, 40 cycles. The PCR products from both amplification conditions were purified and sequenced directly using the primers listed below. Sequence reactions were run in Perkin Elmer 373A Automated Sequencer, and analysed by use of SeqEd and Sequence Navigator software[34]. PCR primers: P9, 5′–GAAGAGGCGGGACTCTTTGACGCGG–3′; 17, 5′–CTTGATGCGGTTGACGGTCTC–3′; 19, 5′–CAAGACCTTTGAGGGCGTTGAC–3′; 13, 5′–TGGTCAGTGGATCAATGAGGTG–3′. Sequencing primers: P10, 5′–GGCCGACGCGCCGCCATCTTT–3′; GD1, 5′–GCAGAAGATGGCAGTGACCAGAGG–3′; GD2, 5′–GAACAAATCAGGTCTGCTGGTAGGAG–3′; GD3, 5′–GTGGAAGTAGCTCCCCAGGTGCCTG–3′; M8, 5′–GCCGAGACTGGAATGTTGACCTG–3′; M9, 5′–GGGAATCAGGTCAACATTCCAGTC–3′; 18, 5′–AAAGCTGCCCTCCACCACCT–3′; GD4, 5′–CCTTATTCTGGACAGCCACCCATC–3′; GD5, 5′–GATCACAGGACAGCTGGGCTGTGAG–3′; GD6, 5′–GGTGAGCCTGTGGCTGAGTACAAG–3′; GD7, 5′–GGTGGGAAGACTGGCCTGGTACCTG–3′; GD8, 5′–CAAGGATGGAGTGAAGTAAATGAAGAGCAC–3′; GD9, 5′–GAGGAAGGGTGCAGTGGAATTGG–3′; GD10, 5′–CAGTCATGACTCTGAAGACTTCTGGAC–3′; GD11, 5′–GCTGCCTGCCCTTGCTGTGAGCG–3′; GD12, 5′–GCAGGGAGCTCCCACACTGATG–3′; GD13, 5′–CTCTGCGTATGGCCAGCGCCTC–3′; 20, 5′–GCAATAGCTATGTACTTGCCCTG–3′; GD15, 5′–CCTGGTCCCTAAGCCCAGCTGC–3′; GD14, 5′–GGATACCTGTCTGACTCACCCTG–3′.

SSCP analysis. SSCP analysis[35] was performed as follows. The 11 exons of the *GDI1* gene were amplified in 10 fragments using the sequencing primer pairs P9/GD1, GD2/M9, GD3/GD4, GD5/GD6, GD7/GD8, GD9/GD10, GD11/GD12, GD13/GD15 and GD14/13. Two additional primers were prepared to amplify exon 10: GD15R (5′–GCAGCTGGGCTTAGGGACCAGG–3′) and GD14R (5′–CAGGGTGAGTCAGACAGGTATCC–3′). PCR products (4 μl of each) were denatured and electrophoresed on 6% polyacrylamide gels (acrylamide/bisacrylamide: 62.5:1) in TBE buffer at RT and 35 W for 3 h. Alternatively, gels containing 10% glycerol were run at 4 °C, for 6–8 h. After electrophoresis, gels were stained for 20 min in 12 mM $AgNO_3$, developed in 0.28 M Na_2CO_3 and 40% formaldehyde, fixed in 10% acetic acid and dried.

Western-blot analysis. Whole cell lysates were fractionated on 10% SDS-PAGE and transferred to nitrocellulose membranes. After incubation with the polyclonal anti-αGDI antibody[21] (1:1000 dilution), the membrane was incubated for 1 h with alkaline phosphatase-conjugated secondary antibody (Promega). Proteins were detected with BCIP/NBT substrate (Promega).

In situ hybridization. Embryos were collected from outbred CD-1 female mice (Charles River) at E8.5–E14.5, fixed over night in 4% paraformaldehyde in PBS and embedded in paraffin. Serial sections of 7 μm were mounted on gelatin coated slides. Brains from older animals (E18.5 and postnatal) were dissected out, fixed over night in 4% paraformaldehyde in PBS, incubated over night in a 20% sucrose gradient at 4 °C, moved to OCT embedding compound (Tissue-Tek), frozen in liquid nitrogen and stored at –70 °C until use. Serial sections (10 μm) were mounted on gelatin-coated slides. When different probes were compared, adjacent sections were used. Two alternative series were used for each probe. Paraffin sections were dewaxed, rehydrated in ethanol, and processed for *in situ* hybridization as described[36].

Probes were prepared by RT-PCR from total RNA from mouse or human brain, reverse transcribed as described using random examers[34]. A fragment of 300 bp of the coding region of *Gdi1* (primers BOV1AH, 5′–TGACCATGGACGAGGAATACGAC–3′ and 18), and a fragment of 500 bp of *Rab3a* (primers RAB1, 5′–ACTCTCGATATGGGCAGAAGGAG–3′ and RAB2, 5′–TGCAAGGTCTGCAGTATCTAGGG–3′) were cloned in Bluescript-T. [γ-^{35}S]-CTP–labelled sense and antisense RNA probes were synthesized with T7 or T3 polymerases (Riboprobe Kit, Promega) from linearized plasmids, and used as described[35]. Autoradiography was performed with Kodak NT/B2 emulsion. Exposure times were between five and twelve days.

Cell cultures. Low density primary cultures of hippocampal neurons were prepared from rat embryos (E18) essentially as described[34]. Cells were maintained in MEM without serum, supplemented with 1% N2 supplement (Life Technologies), 2 mM glutamine, 0.1% BSA, 4 mM glucose, and 1 mM Na-pyruvate. At time zero, antisense oligonucleotides to *Gdi1* mRNA (45 μM) were added to the cultures. At intervals of 12 h, additional oligonucleotides (22 μM) were applied. Two different antisense oligonucleotides were used in different sets of experiments: 5′–CCTTGGTACCAGCGCCCGCTCTTC–3′ (corresponding to the inverse complement of the rat *Gdi1* sequence, nt 51–27) and 5′–CATGGTCAGGCCTTGGTACCAGCGC–3′ (corresponding to the inverse complement of rat *Gdi1* sequence, nt 62–37). The ATG is at nt 60–62.

To measure neurite length, images were acquired directly from coverslips using a Zeiss upright microscope equipped with two digital video cameras (C2400-8 SIT and C2400-7, Hamamatsu). The microscope was connected to a MacIntosh IIci *via* a data translation frame grabber card (DT-2255–50 Hz). The image analysis program NIH Image (http://rsb.nih.gov/nih-image) was used. Different numbers of images were used according to the statistical significance of the results. The total length of processes per cell was determined by measuring all the processes present in a field (from the beginning of the process to the tip, when visible, or to the end of the process on the edge of the image), divided by the number of cell bodies present in the field. The data were statistically analysed using Excel 5.0 (Microsoft).

Double immunofluorescence was carried out as described[37] using monoclonal anti-MAP2 antibodies (Jackson Laboratories) and a rabbit polyclonal anti-αGDI serum[20] followed by Texas-Red conjugated goat anti-rabbit and fluorescein-conjugated goat anti-mouse IgGs (Jackson Laboratories).

Site-directed mutagenesis and analysis of Rab-binding. Point mutations were introduced into bovine *GDI1* by PCR site-directed mutagenesis as described[38]. Sequence-verified mutants were subcloned into the bacterial expression vector pET11d (Novagen) containing a 5′-six histidine tag. After induction with IPTG, mutants were expressed in *E. coli* strain BL21(DE3) and purified on NTA-agarose (Qiagen), followed by Sephacryl S100 and Mono-Q-HR 5/5 (Pharmacia) as described[39]. Propagation of recombinant *Autogapha californica* nuclear polyhedrosis virus (AcMNPV), and growth and expression of RAB3A in Sf9 cells was carried out as described[23]. Prenylated RAB3A was expressed and extracted from *Spodoptera frugiperda* (Sf9) membranes as described[23]. The sample was loaded on a Q-Sepharose Fast Flow (Pharmacia) and eluted by washing the column with buffer A. The fractions containing purified RAB3A were pooled, concentrated five-fold and stored in aliquots at –70 °C. To determine dissociation constants (K_d) for complexes of prenylated RAB3A and

wild-type or mutant αGDI, a range of concentrations (10–50 nM) of prenylated RAB3A were incubated with fixed concentrations of αGDI (100 nM–2 μM) in 200 μl of buffer A (ref. 23) supplemented with 0.1% Lubrol at RT for 1 h. Each sample was applied to a Q-Sepharose Fast Flow column and washed with buffer A (10 ml) to remove free (unbound) RAB3A. Buffer A (1 ml) containing 500 mM NaCl was used to elute GDI-bound RAB3A. Fractions containing the complex were pooled and precipitated with TCA for 2 h. The precipitate was analysed by SDS-PAGE, transferred to nitrocellulose and the amount of RAB3A in the complex was determined using quantitative western blotting with a polyclonal anti-RAB3A antibody as described[23].

RAB3A extraction. Synaptosomes were purified[40] and permeabilized as described[41]. Following incubation with 2 μM αGDI or the indicated mutant for 30 min on ice, membranes were pelleted and the amount of extracted RAB3A determined using quantitative western blotting.

Acknowledgements

We thank P. Willems and A. Meindl for the DNA of patients MRX25 and MRX28, M. Zerial for the gift of the anti-αGDI antibodies, D. Dunlop for help with the computer program, E. Boncinelli for the hospitality to do in situ hybridizations; M. Gatti for skillful technical assistance, K. Zeng for preparation of the illustrations showing structural changes in αGDI and the Galliera Genetic Bank (program C23) for the patient samples. This work was funded by Telethon Italy (D.T. and F.V.) and by GM33301 and EY11606 (W.E.B.).

Received 3 April; accepted 7 May, 1998

1. Lubs, H.A. *et al.* XLMR genes: update 1996. *Am. J. Med. Genet.* **64**, 147–157 (1996).
2. Verkerk, A.J. *et al.* Identification of a gene (*FMR-1*) containing a CGG repeat coincident with a breakpoint cluster region exhibiting length variation in fragile X syndrome. *Cell* **65**, 905–914 (1991).
3. Turner, G., Webb, T., Wake, S. & Robinson, H. Prevalence of fragile X syndrome. *Am. J. Med. Genet.* **64**, 196–197 (1996).
4. Gedeon, A.K., Donnelly, A.J., Mulley, J.C., Kerr, B. & Turner, G. How many X-linked genes for non-specific mental retardation (MRX) are there? *Am. J. Med. Genet.* **64**, 158–162 (1996).
5. Gecz, J., Gedeon, A.K., Sutherland, G.R. & Mulley, J.C. Identification of the gene *FMR2*, associated with FRAXE mental retardation. *Nature Genet.* **13**, 105–108 (1996).
6. Bione, S. *et al.* Transcriptional organization of a 450-Kb region of the human X chromosome, in Xq28. *Proc. Natl. Acad. Sci. USA* **90**, 10977–10981 (1993).
7. Wu, S.K., Zeng, K., Wilson, I.A. & Balch, W.E. Structural insights into the function of Rab GDI superfamily. *Trends Biochem. Sci.* **21**, 472–476 (1996).
8. Pfeffer, S.R., Dirac-Svejstrup, A.B. & Soldati, T. Rab GDP dissociation inhibitor: putting rab GTPases in the right place. *J. Biol. Chem.* **270**, 17057–17059 (1995).
9. Sasaki, T. *et al.* Purification and characterization from bovine brain cytosol of a protein that inhibits the dissociation of GDP from and the subsequent binding of GTP to smg p25A, a ras p21-like GTP-binding protein. *J. Biol. Chem.* **265**, 2333–2337 (1990).
10. Fisher von Mollard, G., Stahl, B., Khokhlatchev, A., Suedhof, T.C. & Jahn, R. Rab3C is a synaptic vesicle protein that dissociates from synaptic vesicle after stimulation of exocytosis. *J. Biol. Chem.* **269**, 10971–10974 (1994).
11. Fischer von Mollard, G., Stahl, B., Li, C., Suedhof, T.C. & Jahn, R. Rab proteins in regulated exocytosis. *Trends Biochem. Sci.* **19**, 164–168 (1994).
12. Wang, Y., Okamoto, M., Schmitz, F., Hofmann, K. & Suedhof, T.C. Rim is a putative Rab3 effector in regulating synaptic-vesicle fusion. *Nature* **388**, 593–598 (1997).
13. Geppert, M. *et al.* The role of Rab3A in neurotrasmitter release. *Nature* **369**, 493–497 (1994).
14. Takai, Y., Sasaki, T., Shirataki, H. & Nakanishi, H. Rab3A small GTP-binding protein in Ca(2+)-dependent exocytosis. *Genes Cells* **1**, 615–632 (1996).
15. Bean, A.J. & Scheller, R.H. Better late than never: a role for rabs late in exocytosis. *Neuron* **19**, 751–754 (1997).
16. Suedhof, T.C. Function of Rab3 GDP-GTP exchange. *Neuron* **18**, 519–522 (1997).
17. Sedlacek, Z., Koneki, B., Korn, B., Klauck, S.M. & Poustka, A. Evolutionary conservation and genomic organization of XA P-4, an Xq28 gene coding for a human rab GDP-dissociation inhibitor (GDI). *Mamm. Genome* **5**, 633–639 (1994).
18. Chen, E.Y. *et al.* Long-range sequence analysis in Xq28: thirteen known and six candidate genes in 219.4 kb of high GC DNA between the *RCP/GCP* and *G6PD* loci. *Hum. Mol. Genet.* **5**, 659–668 (1996).
19. des Portes, V. *et al.* A gene for dominant nonspecific X-linked mental retardation is located in Xq28. *Am. J. Hum. Genet.* **60**, 903–909 (1997).
20. Hamel, B.C.J. *et al.* A gene for non specific X-linked mental retardation (MRX41) is located in the distal segment of Xq28. *Am. J. Med. Genet.* **64**, 131–133 (1996).
21. Ullrich, O. *et al.* Rab GDP dissociation inhibitor as a general regulator for the membrane association of rab proteins. *J. Biol. Chem.* **268**, 18143–18150 (1993).
22. Claes, S. *et al.* X-linked severe mental retardation and a progressive neurological disorder in a Belgian family: clinical and genetic studies. *Clin. Genet.* **52**, 155–161 (1997).
23. Schalk, I. *et al.* Structure and mutational analysis of Rab GDP-dissociation inhibitor. *Nature* **381**, 42–48 (1996).
24. Casey, P.J. & Seabra, M.C. Protein prenyltransferases. *J. Biol. Chem.* **271**, 5289–5292 (1996).
25. Garrett, M.G., Zahner, J.E., Cheney, C.M. & Novick, P.J. Gdi1p encodes a GDP dissociation inhibitor that plays an essential role in the yeast secretory pathway. *EMBO J.* **13**, 1718–1728 (1994).
26. Novick, P. & Zerial, M. The diversity of Rab proteins in vesicle transport. *Curr. Opin. Cell Biol.* **9**, 496–504 (1997).
27. Bachner, D., Sedlacek, Z., Korn, B., Hameister, H. & Poustka, A. Expression patterns of two human genes coding for different rab GDP-dissociation inhibitors (GDIs), extremely conserved proteins involved in cellular transport. *Hum. Mol. Genet.* **4**, 701–708 (1995).
28. Banker, G.A. & Cowan, W.M. Rat hippocampal neurons in dispersed cell culture. *Brain Res.* **126**, 397–352 (1977).
29. Bartlett, W.P. & Banker, G.A. An electron microscopic study of the development of axons and dendrites by hippocampal neurons in culture. II. Synaptic relationships. *J. Neurosci.* **4**, 1954–1965 (1984).
30. Geppert, M., Goda, Y., Stevens, C.F. & Suedhof, T.C. The small GTP-binding protein Rab3A regulates a late step in synaptic vescicles fusion. *Nature* **387**, 810–814 (1997).
31. Castillo, P.E. *et al.* Rab3A is essential for mossy fibre long-term potentiation in the hippocampus. *Nature* **388**, 590–593 (1997).
32. Cremers, F.P.M., van de Pol, T.J.R., van Kerkhoff, L.P.M., Wieringa, B. & Ropers, H.H. Cloning of a gene that is rearranged in patients with choroideremia. *Nature* **357**, 674–677 (1990).
33. Seabra, M.C., Brown, M.S. & Goldstein, J.L. Retinal degeneration in choroideremia: deficiency of rab geranylgeranyl transferase. *Science* **259**, 377–381 (1993).
34. Bione, S. *et al.* Identification of a novel X-linked gene responsible for Emery-Dreifuss muscular dystrophy. *Nature Genet.* **8**, 323–327 (1994).
35. Spinardi, L., Mazars, R. & Theillet, C. Protocols for an improved detection of point mutations by SSCP. *Nucleic Acids Res.* **19**, 4009 (1991)
36. Gulisano, M., Broccoli, V., Pardini, C. & Boncinelli, E. *Emx1* and *Emx2* show different patterns of expression during proliferation and differentiation of the developing cerebral cortex in the mouse. *Eur. J. Neurosci.* **8**, 1037–1050 (1996).
37. Burgaya, F., Menegon, A., Menegoz, M., Valtorta, F. & Girault, J.A. Focal adhesion kinase in rat central nervous system. *Eur. J. Neurosci.* **7**, 1810–1821 (1995).
38. Dascher, C. & Balch, W.E. Dominant inhibitory mutants of ARF1 block endoplasmic reticulum to Golgi transport and trigger disassembly of the Golgi apparatus. *J. Biol. Chem.* **269**, 1437–1448 (1994).
39. Nuoffer, C., Peter, F. & Balch, W.E. Purification of His6-tagged Rab1 proteins using bacterial and insect cell expression systems. *Methods Enzymol.* **257**, 3–8 (1995).
40. Fisher von Mollard, G., Suedhof, T.C. & Jahn R. *Nature* **349**, 79–81 (1991)
41. Dekker, L.V., De Graan, P.N.E., Pijnappel, P., Oestreicher, A.B. & Gispen, W.H. Noradrenaline release from streptolysin O-permeated rat cortical synaptosomes: effects of calcium, phorbol esters, protein kinase inhibitors, and antibodies to the neuron-specific protein kinase C substrate B-50 (GAP-43). *J. Neurochem.* **56**, 1146–1153 (1991)
42. Billuart, P. *et al.* Oligophrenin-1 encodes a rhoGAP protein involved in X-linked mental retardation. *Nature* **392**, 923–926 (1998).